

Lawrence Berkeley National Laboratory

LBL Publications

Title

Probing covalency with oxidant K edge x-ray absorption spectroscopy of UF₄ and UO₂

Permalink

<https://escholarship.org/uc/item/9vb261sc>

Journal

Journal of Vacuum Science & Technology A Vacuum Surfaces and Films, 36(6)

ISSN

0734-2101

Authors

Tobin, JG
Yu, S-W
Qiao, R
et al.

Publication Date

2018-11-01

DOI

10.1116/1.5046947

Peer reviewed

Probing Covalency with Oxidant K Edge

X-ray Absorption Spectroscopy of UF₄ and UO₂

J.G. Tobin^{1*}, S.-W. Yu², R. Qiao³, W.L. Yang³, and D.K. Shuh³

¹*University of Wisconsin-Oshkosh, Oshkosh, WI, USA, 54901;*

²*Lawrence Livermore National Laboratory, Livermore, CA, USA, 94550;*

³*Lawrence Berkeley National Laboratory, Berkeley, CA, USA, 94720*

**Contact email: tobinj@uwosh.edu*

There are some interesting discrepancies between what has been observed experimentally and the predictions of cluster theory. In particular, the F 1s XAS of Uranium Tetrafluoride and the U 4d XAS branching ratio (BR) for oxidized uranium are two cases in point. These discrepancies may be driven by the overestimation of covalency in cluster calculations.

I INTRODUCTION

Over the course of the last several years, cluster calculations have been used in a myriad of ways to analyze spectroscopic results from actinide systems and gain insight into the electronic structure of these actinide systems. For example, the calculated 6d Unoccupied Density of States (UDOS) in Uranium Tetrafluoride (UF₄) and Uranium Dioxide (UO₂) were probed using U L₃ (2p_{3/2} → 6d) X-ray Absorption Near Edge Structure (XANES) as well as U N₇ (4f_{7/2} → 6d) X-ray Absorption Spectroscopy (XAS). [1-3] Cluster calculations have also been used successfully to study the development from atomic to bulk electronic structure in Pu [4,5]

and issues associated with the 2p Occupied Density of States (ODOS) in Uranium Tetrafluoride. [6, 7] However, there now appear to be some interesting discrepancies between what has been observed experimentally and the predictions of cluster theory: In particular, the F 1s XAS of Uranium Tetrafluoride [8] and the U 4d XAS branching ratio (BR) for oxidized uranium. [1] These issues will be addressed below.

II. EXPERIMENTAL

The central thrust of this work will be an examination of the F K ($1s \rightarrow 2p$) and O K ($1s \rightarrow 2p$) transitions in X-ray Absorption Spectroscopy. (Figures 1 and 2) The X-ray Absorption Spectroscopy measurements were carried out at beamline (BL) 8.0 at the Advanced Light Source (ALS) at Lawrence Berkeley National Laboratory (LBNL). For BL 8.0, energy calibrations were performed at the Fe $2p_{3/2}$ white line (710 eV for iron oxide) for the beamline monochromator. Here, the XAS energy scale will be expressed relative the threshold energy, as defined in References 8, 9 and 10. Details of the BL 8.0 characteristics can be found in Reference 11. Data were collected at room temperature (~ 300 K). The uranium tetrafluoride was a single-crystalline sample, with significant surface degradation, but by using Total Fluorescence Yield (TFY) detection, it was possible to sample the true bulk UF_4 transitions. [6, 8, 12].

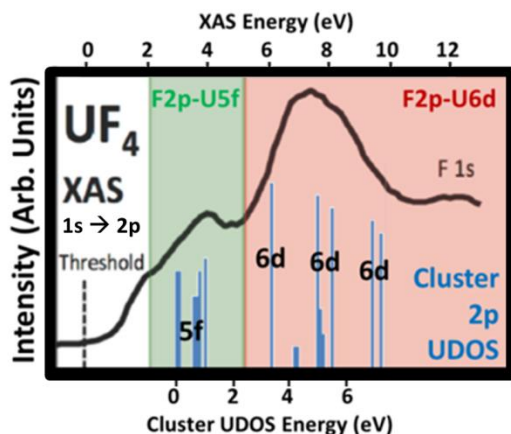
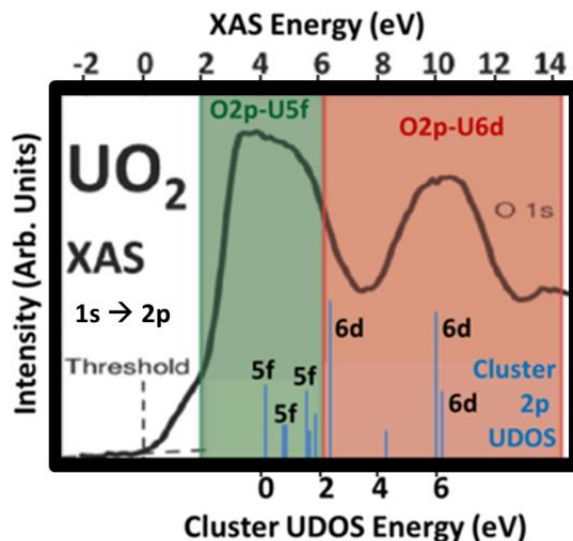


Figure 1. (Color Online) XAS versus the F2p UDOS from the Ryzhkov cluster calculation.[3] In the low energy manifold, all of the states have strong 5f character. In the high energy manifold, the five large histogram peaks each have strong 6d character. There are also a few weaker peaks with no 6d contribution. [Reprinted/Adapted] from A. Yu. Teterin, Yu. A. Teterin, K. I. Maslakov, A. D. Panov, M. V. Ryzhkov, and L. Vukcevic, Phys. Rev. B 74, 045101 (2006). Copyright 2006 by the American Physical Society.

Figure 2. (Color Online) XAS versus the O2p UDOS from the Ryzhkov cluster calculation [2]. Similar to Figure 1. Re-used with permission from J.G. Tobin, S.-W. Yu, R. Qiao, W.L. Yang, and D.K. Shuh, "F1s X-ray Emission Spectroscopy of UF4," Progress in Nuclear Science and Technology, (to be published). [Reprinted/Adapted] from Yu. A. Teterin, K. I. Maslakov, M. V. Ryzhkov, O. P. Traparic, L. Vukcevic, A. Yu. Teterin, and A. D. Panov, Radiochemistry 47, 215 (2005). Copyright 2005 by Springer.



The X-ray Absorption process is shown schematically in Figure 3. Because core level electrons are involved in these processes, there is a fundamental elemental specificity to the analysis. By comparison with the placement of other spectroscopic features, including U4d and U4f XAS, it is possible to further subdivide the K ($1s \rightarrow 2p$) absorption into regions associated with U5f and U6d UDOS. These comparisons involve extensive cross calibration of energy scales and the utilization of multiple, overlapping techniques. [8, 9, 13] These prior determinations are shown as green (2p-U5f) and red (2p-U6d) shaded ranges in Figures 1 and 2.

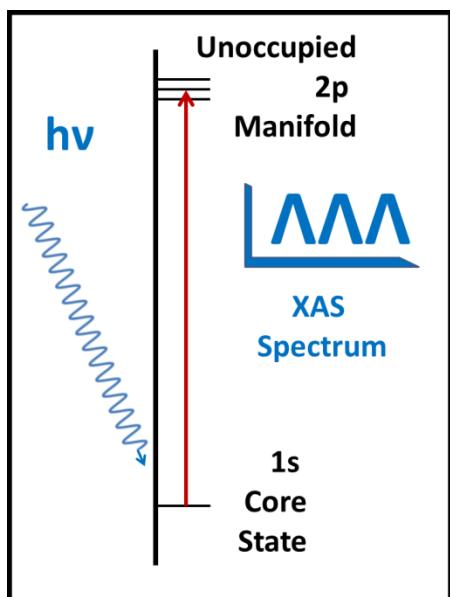


Figure 3 (Color online)
Schematic of the $1s \rightarrow 2p$
XAS process.

III. Results and Discussion

A. Comparison to Cluster Theory

Ai. Cluster Histograms

The initial comparison between the XAS results and the predictions of cluster theory are shown in Figures 1 and 2. Here, the energies of the empty states were extracted from References 2 and 3 and a histogram plotted, at each energy, with the height of the histogram corresponding to the percentage of 2p nature of that state and, of course, scaled to degeneracy. The energy scales of the XAS and cluster calculations are each fixed internally but allowed to slide relative to each other, with the degree of shift corresponding to a maximization of agreement between the XAS peaks and the cluster theory histograms. The results of these operations are shown in Figures 1 and 2 and significantly good agreement is achieved, with 2p-5f histograms in the green regions and 2p-6d-histograms in the red. Thus, on some fundamental level, there is sound agreement between the cluster calculations of the 2p Unoccupied Density of States (2p UDOS) and the XAS measurements, including the nature of the hybridization with U5f and U6d unoccupied states.

Aii. Simulated Spectra with Gaussian Peak-shapes

A more stringent comparison would be to generate simulated spectra by substituting a scaled peakshape for each histogram. The K (1s) XAS spectrum is the result of a transition of an electron from an occupied 1s state into a 2p hole, as shown schematically in Figure 3. These transitions will be electric dipole in nature, with $\Delta l = \pm 1$. For each state in the UDOS manifold with 2p character, there should be a corresponding peak in the XAS spectrum, with a finite width caused by a variety of factors, including lifetime broadening and instrumental resolution

limitations, as illustrated in Figure 3. The approach here is to take each unoccupied state in the Ryzhkov cluster calculation with non-zero 2p character and generate an XAS component peak for it, scaling the intensity to the 2p percentage, and then sum all of the component peaks to get an overall spectrum. For the sake of simplicity and transparency, a Gaussian function will be utilized as the component line-shape. The results of this approach are shown in Figure 4, for a series of component Full-Widths-At-Half-Maxima (FWHM). Within each simulated spectrum, constant cross sections and component widths and shapes will be assumed throughout.

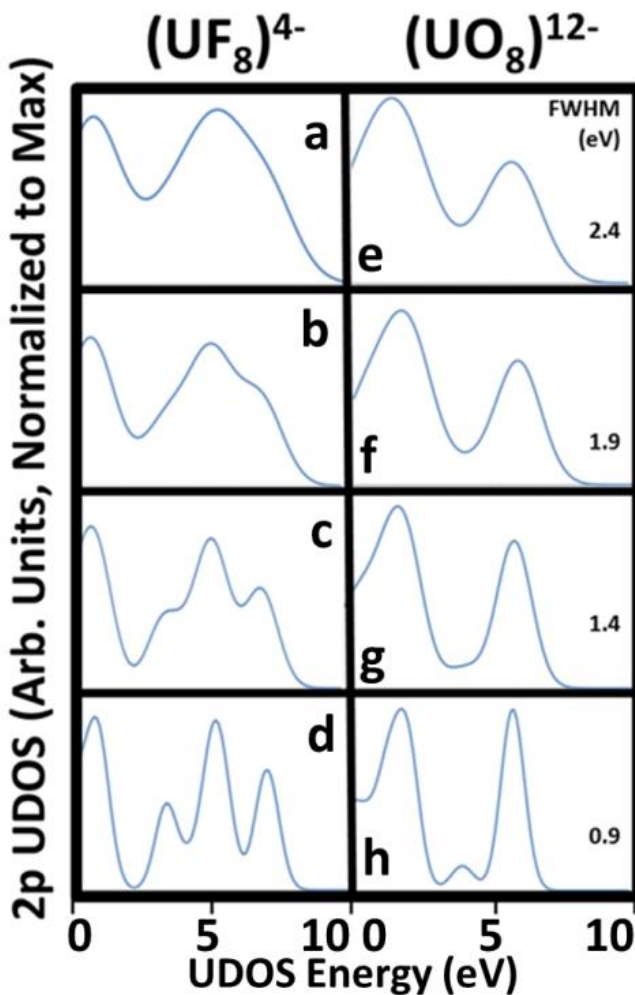


Figure 4 (Color online) Simulated XAS spectra from the cluster histograms, as described in the text. The FWHM of the components are varied from 0.9 eV to 2.4 eV, as follows. For $(UF_8)^{4-}$: (a) 2.4, (b) 1.9, (c) 1.4, (d) 0.9. For $(UO_8)^{12-}$: (e) 2.4, (f) 1.9, (g) 1.4, (h) 0.9.

For Uranium Dioxide, the comparison between the experimental XAS results and the simulated spectrum with $FWHM = 2.4$ eV exhibits fairly good agreement, as shown in Figure 5.

Here, the shifted energy scales remain fixed to the values found in Figure 3. The doublet structure of the XAS is reconstructed in the simulated spectrum, with a pure 2p-6d peak at higher energies and a mixed 2p-5f and 2p-6d peak at lower energies.

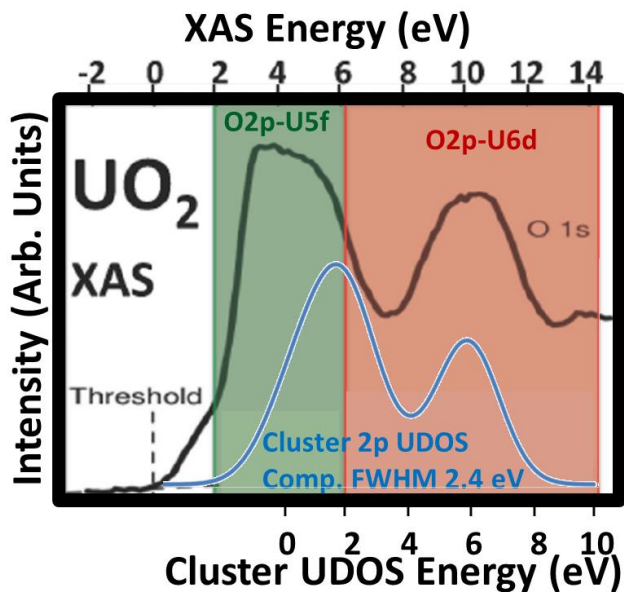
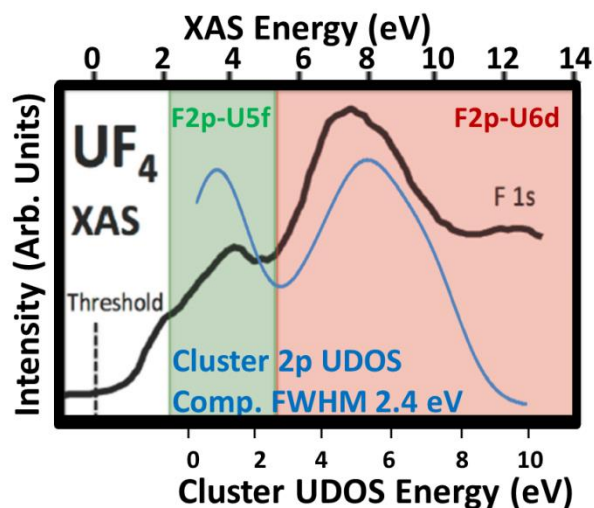


Figure 5 (Color Online)
The comparison of the O K ($1s \rightarrow 2p$) XAS spectrum (black) of UO_2 to the simulated spectrum from the $(\text{UO}_8)^{12-}$ cluster (blue). The simulated spectrum has been extended below 0 to enhance the comparison. The vertical scaling is arbitrary.

However, the comparison for the Uranium Tetrafluoride does not show such agreement.

(Figure 6) Next, the cause of the disagreement will be discussed.

Figure 6 (Color online)
The comparison of the F K ($1s \rightarrow 2p$) XAS spectrum (black) of UF_4 to the simulated spectrum from the $(\text{UF}_8)^{4-}$ cluster (blue). The vertical scaling is arbitrary.



Aiii. Simulated Spectra with Gaussian Peak-shapes and Step-Functions

Visual inspection of Figure 6 indicates that the lower energy feature looks more like a step than a peak. The question then arises: when might it be expected to see a step instead of a peak? In measurements such as Photoelectron Spectroscopy (PES) [14] and Inverse Photoelectron Spectroscopy (IPES) [15], steps are often observed at the Fermi Edge or the threshold for a large density of states. An example of this is shown in Figure 7, where the Inverse Photoelectron Spectra of Ge (111) at a series of incident angles is plotted. The step corresponds to the onset of a relatively large density of unoccupied states, i.e UDOS. There are potentially many unresolved states here, some dispersing with momentum (energy versus angle), sampled by Direct and Indirect Transitions, that coalesce into a step like feature. [14,15]

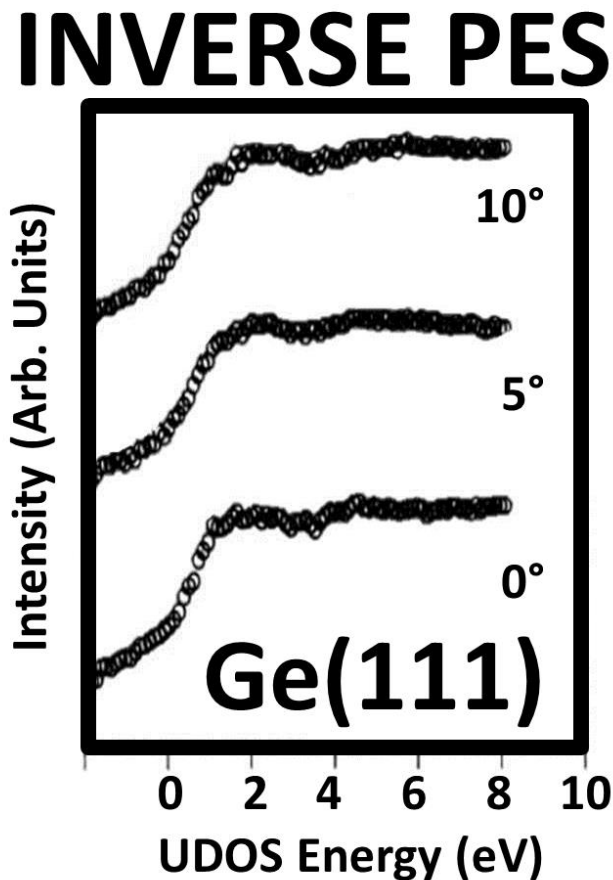


Figure 7. Shown here is the Inverse Photoelectron Spectroscopy (IPES) of Ge(111). The spectra were collected with the electron momentum in the I-M azimuthal plane of the 1X1 Ge{111} Surface Brillion Zone, with the electrons (excitation) incident at angles of 0°, 5°, and 10° versus the surface normal. Note the step-like appearance of all three spectra. [Reprinted/Adapted] from B. Knapp and J. Tobin, Phys. Rev. B 37, 8656 (1988). Copyright 1988 by the American Physical Society.

An advantage of using Gaussian Functions is that it is possible to properly scale the Gaussian Step Function to the Gaussian Peak Function. Following this procedure and substituting Gaussian Step Functions for the 2p-5f histograms, the result obtained is illustrated in Figure 8. Clearly, the agreement has been greatly enhanced. In light of the Ge results in Figure 7, this observation suggests that the 5f states are not being captured and hybridized into covalent bonds with the empty F2p states, possibly instead becoming slightly delocalized.

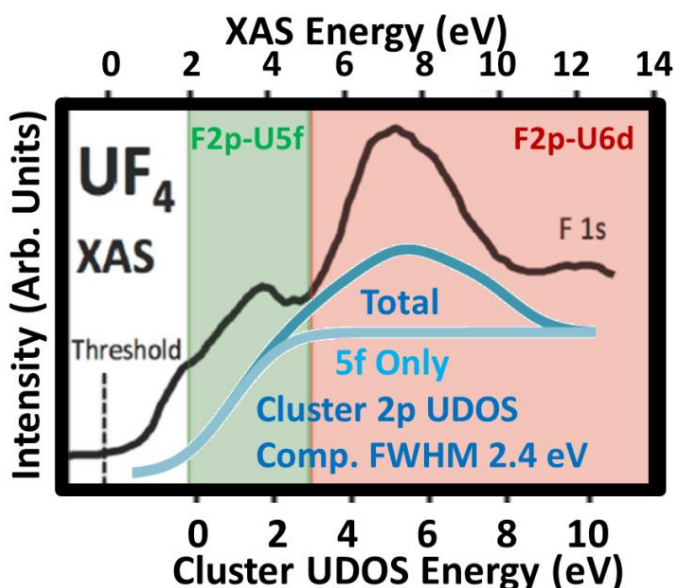


Figure 8 (Color online) The comparison of the F K ($1s \rightarrow 2p$) XAS spectrum (black) of UF_4 to the simulated spectrum from the $(UF_8)^{4-}$ cluster (blue), with 2p-5f histograms treated as steps and the other 2p histograms treated as peaks. The simulated spectrum has been extended below 0 to enhance the comparison. The vertical scaling is arbitrary.

There are many ways to treat the underlying step-like features in XAS. This includes step-functions and asymmetric lineshapes such as Doniach-Sunjic functions. However, our discussion is not particularly concerned about the presence of underlying steps but rather the presence and absence of the whitelines that are predicted by the cluster theory. The cluster theory correctly predicts whitelines for the 2p-6d empty states in UF_4 and the 2p-6d and 2p-5f empty states in UO_2 . However, the theory incorrectly predicts a strong whiteline for the 2p-5f empty states in UF_4 . The absence of the 5f-2p whiteline in UF_4 is then shown to correlate with the large step-like function that is observed experimentally and can possibly be associated with 5f delocalization, in analogy with the step-like spectra in IPES.

IV. Summary and Conclusions

From extensive earlier experimental measurements [8, 9, 13], it had already been demonstrated that the 5f electrons of UF_4 are far less covalent than the 5f electrons of UO_2 . Here, it has been shown that the UF_4 cluster calculations underestimate the degree of 5f isolation from the $\text{F}2p$'s, thus generating results consistent with too much covalency in the 5f's. This too, is not unexpected, since cluster calculations are intrinsically biased away from delocalization and the 5f isolation may be associated with delocalization. However, there is a very important corollary for this result: it explains another discrepancy between XAS and cluster calculations. [1]

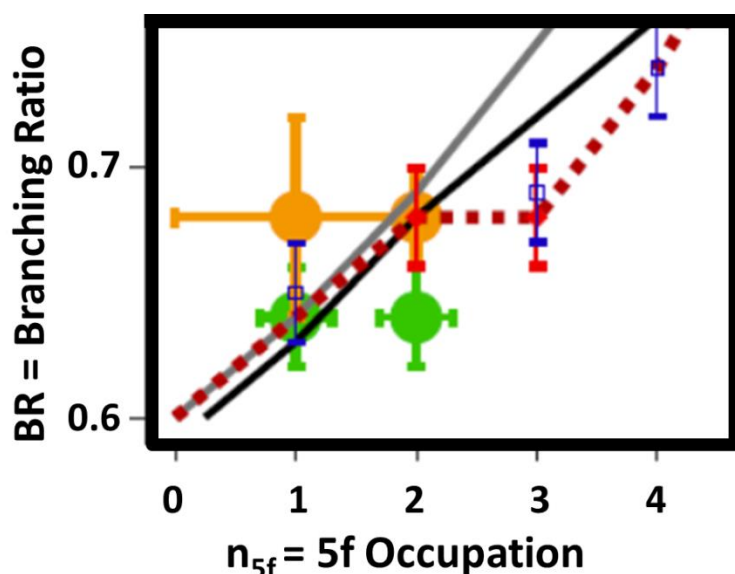


Figure 9. (Color Online) A summary of BR versus 5f occupation. (See Ref 1 for details.) The jj limit curve is a solid gray line. The solid black line is the intermediate model result. The experimental results, shown typically with error bars of ± 0.02 , are from XAS (filled red diamonds), EELS (hollow blue squares), and UO_2 -STXM, $n_{5f} \approx 2$ and UO_3 -STXM, $n_{5f} \approx 1$ (both: filled orange circle with error bars). The results from cluster calculations for UO_2 ($n_{5f} \approx 2$) and UO_3 ($n_{5f} \approx 1$) are shown as filled green circles with error bars. EELS is Electron Energy Loss Spectroscopy. STXM is Scanning X-ray Transmission Microscopy. [Reprinted/Adapted] from J. G. Tobin, S.-W. Yu, C. H. Booth, T. Tyliczszak, D. K. Shuh, G. van der Laan, D. Sokaras, D. Nordlund, and T.-C. Weng, and P. S. Bagus, Phys. Rev. B 92, 035111 (2015). Copyright 2015 by the American Physical Society.

The Branching Ratios of the integrated intensities in the in the 4d to 5f transitions of the actinide elements has provided great insight into the 5f electronic structure of these elements, particularly the localized cases. [1] However, some discrepancies remain. The cluster calculation predictions for the BR (green circles) are consistently lower than the experimental results (orange circles). The over-application of perturbations with the symmetry of the crystal field (CF) could be driving this, since CF symmetry effects will tend to lower the BR towards the statistical value of $BR = 0.6$. It appears that the cluster theory, with no delocalization, overemphasizes CF symmetry and covalency.

Acknowledgements

Lawrence Livermore National Laboratory (LLNL) is operated by Lawrence Livermore National Security, LLC, for the U.S. Department of Energy, National Nuclear Security Administration, under Contract DE-AC52-07NA27344. Work at Lawrence Berkeley National Laboratory (LBNL) (D.K.S.) was supported by the Director of the Office of Science, Office of Basic Energy Sciences (OBES), Division of Chemical Sciences, Geosciences, and Biosciences (CSGB), Heavy Element Chemistry (HEC) Program of the U.S. Department of Energy under Contract No. DE-AC02-05CH11231. The ALS is supported by the Director of the Office of Science, OBES of the U.S. Department of Energy at LBNL under Contract No. DE-AC02-05CH11231. The UF_4 sample was originally prepared at Oak Ridge National Laboratory and provided to LLNL by J. S. Morrell of Y12.

References

1. J. G. Tobin, S.-W. Yu, C. H. Booth, T. Tyliczszak, D. K. Shuh, G. van der Laan, D. Sokaras, D. Nordlund, and T.-C. Weng, and P. S. Bagus, *Phys. Rev. B* **92**, 035111 (2015).

2. Yu. A. Teterin, K. I. Maslakov, M. V. Ryzhkov, O. P. Traparic, L. Vukcevic, A. Yu. Teterin, and A. D. Panov, *Radiochemistry* **47**, 215 (2005).
3. A. Yu. Teterin, Yu. A. Teterin, K. I. Maslakov, A. D. Panov, M. V. Ryzhkov, and L. Vukcevic, *Phys. Rev. B* **74**, 045101 (2006).
4. M. V. Ryzhkov, A. Mirmelstein, S.-W. Yu, B. W. Chung, and J. G. Tobin, *International Journal of Quantum Chemistry* **113**, 1957 (2013).
5. M.V. Ryzhkov, A. Mirmelstein, B. Delley, S.-W. Yu, B.W. Chung, J.G. Tobin, *Journal of Electron Spectroscopy and Related Phenomena* **194**, 45 (2014).
6. J.G. Tobin, S.-W. Yu, R. Qiao, W.L. Yang, and D.K. Shuh, "F1s X-ray Emission Spectroscopy of UF₄," *Progress in Nuclear Science and Technology* (to be published).
7. Elisabeth Thibaut, Jean-Pol Boutique, Jacques J. Verbist, Jean-Claude Levet and Henri Noel, *J. Am. Chem. Soc.* **104**, 5266-5273 (1982).
8. J. G. Tobin, S.-W. Yu, R. Qiao, W. L. Yang, C. H. Booth, D. K. Shuh, A. M. Duffin, D. Sokaras, D. Nordlund, and T.-C. Weng, *Phys. Rev. B* **92**, 045130 (2015).
9. S.-W. Yu, J. G. Tobin, J. C. Crowhurst, S. Sharma, J. K. Dewhurst, P. Olalde-Velasco, W. L. Yang, and W. J. Siekhaus, *Phys. Rev. B* **83**, 165102 (2011).
10. S.-W. Yu, J. G. Tobin, P. Olalde-Velasco, W. L. Yang, and W. J. Siekhaus, *J. Vac. Sci. Tech. A* **30**, 011402 (2012).
11. J. J. Jia, T. A. Callcott, J. Yurkas, A. W. Ellis, F. J. Himpsel, M. G. Samant, J. Stohr, D. L. Ederer, J. A. Carlisle, E. A. Hudson, L. J. Terminello, D. K. Shuh, and R. C. C. Perera, *Rev. Sci. Instrum.* **66**, 1394 (1995).
12. J. G. Tobin, A. M. Duffin, S.-W. Yu, R. Qiao, W. L. Yang, C. H. Booth, and D. K. Shuh, *J. Vac. Sci. & Tech. A* **35**, 03E108 (2017)
13. J.G. Tobin and S.-W. Yu, *Phys. Rev. Lett.* **107**, 167406 (2011).
14. J. Nelson, S. Kim, W. Gignac, R. Williams, J. Tobin, S. Robey and D. Shirley, *Phys. Rev. B* **32**, 3465 (1985).
15. B. Knapp and J. Tobin, *Phys. Rev. B* **37**, 8656 (1988).